J. Plasma Fusion Res. SERIES, Vol. 5 (2002) 302–305

Hydrogen Plasma Production in the Lower-Hybrid Frequency Range

KIKUCHI Hideki, SAKAWA Youichi and SHOJI Tatsuo

Department of Energy Engineering and Science, Nagoya University, Nagoya 464-8603, Japan

(Received: 17 December 2001 / Accepted: 5 July 2002)

Abstract

Hydrogen plasmas are produced by using the radio frequency (rf) discharge. Plasma density n_p depends strongly on the strength of the external magnetic field B_0 and has a peak when B_0 and the frequency satisfy the lower-hybrid resonance condition. Various types of antennas are used, and the helical antenna gives the maximum n_p of 5×10^{12} cm^{-3} at 3.5 kW and 200 G.

Keywords:

hydrogen plasma, lower hybrid resonance, antenna configuration, loop antenna, helical antenna

1. Introduction

Compact high-density hydrogen beam sources are useful for measuring local ion and electron temperatures and densities in nuclear fusion research. Plasma production by using wave electric field in the frequency range of $\omega_{ci} \ll \omega \ll \omega_{ce}$ is known as a helicon-wave discharge. Helicon-wave plasma sources are attractive because they can produce high-density plasmas at relatively low gas pressure of a few mTorr [1-3]. However, when hydrogen gas is used, plasma density is low compared with rare-gas plasmas [4]. Our purpose is to develop a compact high-density hydrogen-plasma source by using radio frequency (rf) discharges. In this study, plasma production near the lower-hybrid resonance condition is investigated. Various types of antennas are used and optimization of antenna structure is conducted.

2. Experimental Setup

The experiment is conducted in a linear device shown in Fig. 1. A vacuum chamber is made of stainless steal (inner diameter is 36.5 cm and length is 150 cm). A Pyrex tube with inner diameter of 5 cm and length of 90 cm is connected to one end of the vacuum chamber. The maximum magnetic field strength (B_0) on the chamber axis is 1400 G within 5 % uniformity in the plasma region. Hydrogen gas is used in the pressure P_0 = 9.1 mTorr, and the flow rate is 20 sccm. An rf (power P_{rf} < 4.5 kW and frequency f = 13.56 ~ 28.4 MHz) is pulse modulated (pulse length = 3 ms and repetition time = 67 ms) and applied to antennas wound on the Pyrex tube. Radially-movable Langmuir probes are placed at z = 3 and 40 cm. The plasma density n_p is measured from the ion saturation current of the probe at

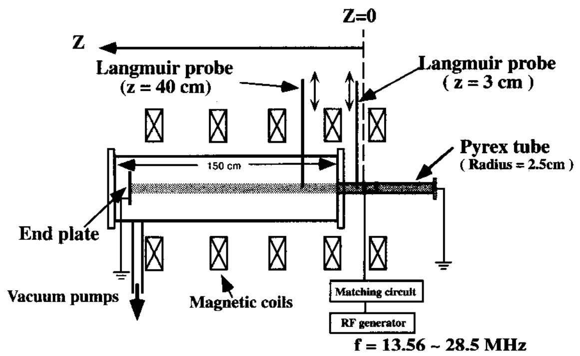

Fig. 1 Schematic view of the experiment setup.

Corresponding author's e-mail: h-kikuchi@ees.nagoya-u.ac.jp

$z = 3$ cm. Here, $z = 0$ is the position of the antenna edge. The electron temperature T_e is measured by the probe at $z = 40$ cm, which accomplishes an rf compensation [5].

3. Antenna Configurations

Figure 2 shows three types of antennas that are used to examine efficiency of hydrogen plasma production. All antennas are made of a copper strip. One is the helix type [Fig. 2(a)], in which the rf current flows with a pitch angle θ with respect to B_0. The copper strip is wound along the Pyrex tube and its length on the surface of the tube is kept constant with 11 cm. When $\theta = 0$, the antenna is identical to Nagoya type III antenna [6], and induces the rf electric field parallel to B_0, E_z, in vacuum. As θ increases, both E_z and the azimuthal component of the electric field E_θ are induced. When $\theta = 90°$, the antenna is nearly a half-turn loop antenna. The antenna induces mainly E_θ, and E_z in vacuum vanishes. In Fig. 2(b) a two-turn loop antenna is shown. L and W are defined as the distance between two antenna loops and width of antenna strip, respectively. Figure 2(c) shows a helical type antenna, in which the length along B_0 and the helical pitch is 20 cm and 23°, respectively. This antenna induces both E_θ and E_z components.

4. Results

The variation of n_p as a function of P_{rf} for $B_0 = 0$ and 200 G with the two-turn loop antenna ($L = 0$ cm and $W = 1$ cm) and for $B_0 = 150$ G with the one-turn loop antenna ($W = 1$ cm) is shown in Fig. 3(a). Density jumps, which mean discontinuous increase in n_p as P_{rf} increases, occur at 500 W and 1.5 kW when $B_0 = 0$ and 200 G, respectively. We define the discharge modes before and after the density jump as the low-density (LD) mode and the high-density (HD) mode, respectively. When $B_0 = 0$ G, in the LD mode the plasma production is done by the electric field due to the antenna voltage V_{rf} (E discharge), on the other hand, in the HD mode plasma is produced by the electric field due to the antenna current I_{rf} (H discharge) [7]. When $B_0 = 200$ G, even though the threshold P_{rf} is larger than that for $B_0 = 0$ G, the density jump corresponds to the transition from E to H discharge. In the LD mode, n_p for the one-turn loop antenna is smaller than that for the two-turn loop antenna because of the smaller V_{rf} due to its lower inductance. When the one-turn loop antenna is used, the density jump or the transition from E to H discharge does not occur. This is because the induction field for the one-turn loop antenna is half of that for the two-turn one.

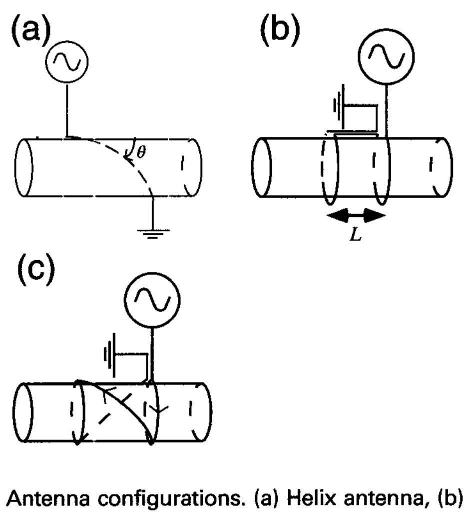

Fig. 2 Antenna configurations. (a) Helix antenna, (b) two-turn loop antenna and (c) helical antenna.

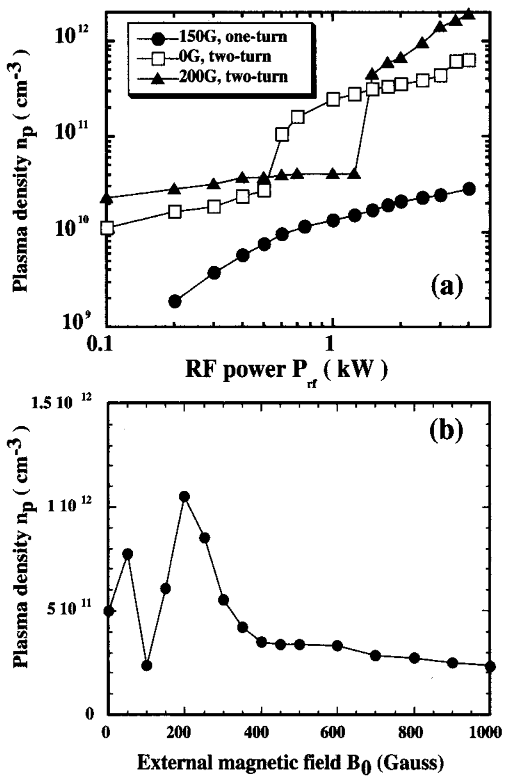

Fig. 3 (a) Dependence of n_p on P_{rf} with and without B_0 using the two-turn ($L = 0$ cm and $W = 1$ cm) and one-turn loop antennas ($W = 1$ cm). (b) Plasma density n_p versus B_0 using the two-turn loop antenna ($L = 0$ cm and $W = 1$ cm) at the HD mode ($P_{rf} = 3$ kW).

Figure 3(b) shows the dependence of n_p on B_0 for the two-turn loop antenna at the HD mode ($P_{rf} = 3$ kW). n_p peaks around 200 G, where the lower-hybrid resonance condition $\omega = \omega_{LH}$ is satisfied. Here, ω_{LH} is defined by the following equation,

$$\omega_{LH}^2 = \omega_{ce}\omega_{ci}\left(\frac{\omega_{pe}^2 + \omega_{ce}\omega_{ci}}{\omega_{pe}^2 + \omega_{ce}^2}\right), \qquad (1)$$

where ω_{ce} and ω_{ci} are the electron and ion cyclotron frequencies, respectively, and ω_{pe} is the electron plasma frequency. At the high-density limit of $\omega_{pe}^2 \gg \omega_{ce}^2 \gg \omega_{ce}\omega_{ci}$, ω_{LH} is given by

$$\omega_{LH-HD} = \sqrt{\omega_{ce}\omega_{ci}}\,. \qquad (2)$$

Nearly two times larger n_p at $B_0 = 200$ G than that at $B_0 = 0$ G is caused by the contribution of the high-efficient plasma production at the lower hybrid resonance in addition to H discharge.

The dependence of n_p on B_0 is measured as a function of f using the two-turn loop antenna ($L = 10$ cm and $W = 3$ cm) at the HD mode $P_{rf} = 1$ kW). When f is varied, n_p peaks at different values of B_0 that satisfy the lower-hybrid resonance condition, and reaches $n_p \simeq 6 \times 10^{11}$ cm^{-3}. Figure 4 shows B_0 at the peak of n_p, B_p, versus f. The calculated B_0 that satisfies $\omega = \omega_{LH-HD}$, B_{LH-HD}, is also shown. The measured B_p shows similar f dependence to B_{LH-HD}. The difference between B_p and B_{LH-HD} can be explained by considering the contribution of the plasma density shown in eq. (1).

The plasma density n_p versus B_0 for $\theta = 0°$, 27° and 90° of the helix antennas at $P_{rf} = 3$ kW is shown in Fig. 5(a). When $\theta = 27°$, n_p peaks strongly near the lower hybrid resonance and the discharge is in the HD mode. While when $\theta = 0°$, the density peak around the lower hybrid resonance is not observed. When $\theta = 90°$, the discharge is in the LD mode because of low induction field.

Figure 5(b) shows n_p at $B_0 \simeq 200$ G, i.e., near the lower-hybrid resonance condition, as a function of θ. The plasma density n_p peaks at $\theta \simeq 45°$. When $\theta > 70°$, n_p values are small and the discharges are in the LD mode.

The dependence of n_p on B_0 at the HD mode ($P_{rf} = 3.5$ kW) with the helical antenna, which has the both E_z and E_θ [see Fig. 2(b)], is shown in Fig. 6. The maximum density of 5×10^{12} cm^{-3} is achieved at 200 G. Furthermore, $n_p > 1.6 \times 10^{12}$ cm^{-3} is obtained in a wide B_0 range of $B_0 = 100 \sim 900$ G.

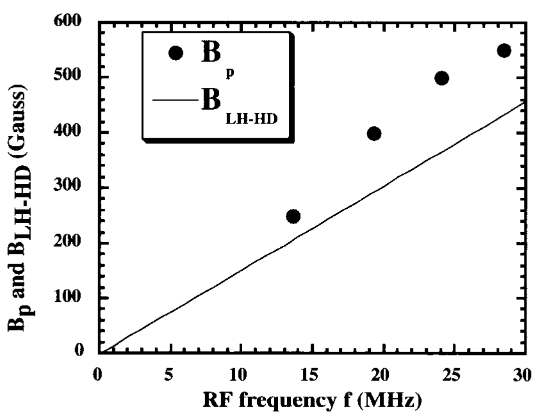

Fig. 4 RF frequency f dependence of the measured B_p at the HD mode ($P_{rf} \simeq 1$ kW) using the two-turn loop antenna (L =10 cm and W = 3 cm) and the calculated B_{LH-HD}.

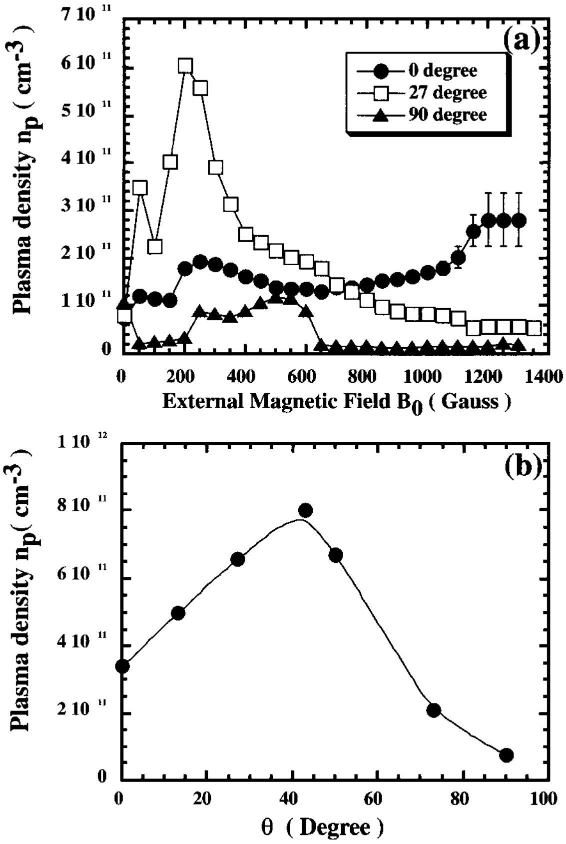

Fig. 5 (a) Plasma density n_p versus B_0 for $\theta = 0°$, 27° and 90° of the helix antennas at $P_{rf} = 3$ kW. (b) Plasma density n_p around the lower-hybrid resonance condition ($B_0 \simeq 200$ G) as a function of θ at $P_{rf} = 3$ kW.

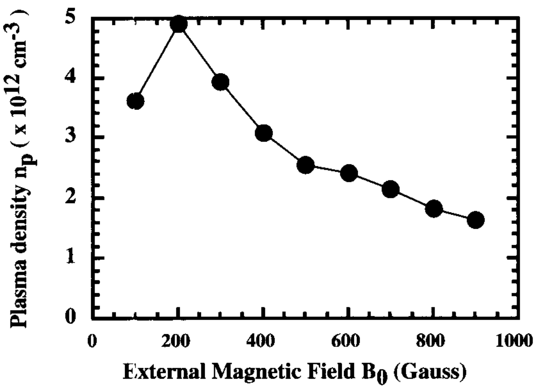

Fig. 6 Plasma density n_p versus B_0 with the helical antenna at P_{rf} = 3.5 kW.

5. Discussion

The dispersion relation of electromagnetic waves in a uniform plasma is expressed as [8]

$$Sn_\perp^4 + [n_{//}^2 (S + P) - (RL + PS)]n_\perp^2 + P(n_{//}^2 - R)(n_{//}^2 - L) = 0, \quad (3)$$

where $n_\perp = ck_\perp/\omega$, $n_{//} = ck_{//}/\omega$, c is the speed of light, and $k_\perp$ ($k_{//}$) is the wave number perpendicular (parallel) to B_0, respectively. R, L, P, S and D are the dielectric tensor elements [8]. When $\omega_{ci} \ll \omega \ll \omega_{ce}$, two branches exist; one is the slow waves and the other is the fast waves (helicon waves) [4]. The slow and fast waves exist in the low-density and high-density regions, respectively. When $B_0 < B_{LH-HD}$, the slow and fast waves merge each other at $N_z^2 \simeq 4S$. On the other hand, when $B_0 > B_{LH-HD}$ the slow waves satisfy the lower hybrid resonance at $S = 0$. In the density region below 10^{12} cm^{-3}, it is difficult to excite the helicon waves since the axial wavelength becomes too long compared with the plasma length. Therefore, enhancement of n_p at the lower hybrid resonance in this density region might be caused by the slow waves.

Near the lower hybrid resonance, the dispersion relation of the slow waves is identical to that of the cold electrostatic waves, and the slow waves propagate almost perpendicular to B_0 in the radial direction [4]. Therefore, as approaching to the resonance the radial component of the electric field E_r becomes large. In order to make the antenna field couple effectively to the waves near the resonance, antennas producing large E_r should be used. Therefore, it seems that $\theta = 0°$ antenna which induces large E_z in vacuum is not appropriate to excite the wave electric field near the resonance and no enhancement of n_p occurs as shown in Fig. 5(a). If the loop antennas having E_θ component are used, the production of the space charge is possible due to the radial motion of electrons caused by $E_\theta \times B_0$ drift. The resultant radial electrostatic fields couple to the slow waves near the lower hybrid resonance as shown in Figs. 3(b) and 4.

When the helical antenna is used, the maximum n_p of 5×10^{12} cm^{-3} is achieved at B_0 = 200 G, and $n_p > 1.6 \times 10^{12}$ cm^{-3} is obtained for B_0 = 100 ~ 900 G. According to the results shown in Figs. 5 and 6, the antennas having both E_θ and E_z, such as the 27° antenna and the helical antenna, are effective to produce high-density hydrogen plasmas. Especially, the helical antenna is suitable to excite the helicon waves with azimuthal mode $m = +1$ [3]. Therefore, it is likely that the helicon waves start to contribute to the plasma production in this density region in addition to that of the slow waves.

In order to clarify the contribution of waves on the plasma production, we are planning to measure the wave magnetic field using a magnetic probe.

6. Conclusion

Hydrogen-plasma production using the rf discharge in the frequency range of $\omega_{ci} \ll \omega \ll \omega_{ce}$ is investigated. Plasma density n_p peaks when B_0 satisfies the lower-hybrid resonance condition. The dependence of n_p on the pitch angle (θ) is measured using the helix type antennas. E_z and E_θ are necessary for efficient hydrogen plasma production. The maximum values of n_p obtained at 3.5 kW are 5×10^{12} cm^{-3} for the helical antenna, 1.7×10^{12} cm^{-3} for the two-turn loop antenna and 7×10^{11} cm^{-3} for the helix antenna.

References

[1] R.W. Boswell, Plasma Phys. Control. Fusion **26**, 1147 (1984).

[2] F.F. Chen, Plasma Phys. Control. Fusion **33**, 364 (1991).

[3] T. Shoji, Y. Sakawa, S. Nakazawa, K. Kadota and T. Sato, Plasma Sources Sci. Technol. **2**, 5 (1993).

[4] Y. Sakawa, T. Takino and T. Shoji, Phys. Plasmas **6**, 4759 (1999).

[5] I.D. Sudit and F.F. Chen, Plasma Sources Sci. Technol. **3**, 162 (1994).

[6] T. Watari *et al.*, Phys. Fluids **21**, 2076 (1978).

[7] A. Degeling, N. Mikhelson, R. Boswell and N. Sadeghi, Phys. Plasmas **5**, 572 (1998).

[8] T.H. Stix, *The Theory of Plasma Waves* (McGraw-Hill, New York, 1962).